nature photonics

LETTERS

PUBLISHED ONLINE: 6 JUNE 2016 | DOI: 10.1038/NPHOTON.2016.105

Phase-coherent microwave-to-optical link with a self-referenced microcomb

Pascal Del'Haye[1,2]*, Aurélien Coillet[2†], Tara Fortier[2], Katja Beha[2], Daniel C. Cole[2], Ki Youl Yang[3], Hansuek Lee[3†], Kerry J. Vahala[3], Scott B. Papp[2] and Scott A. Diddams[2]*

Precise measurements of the frequencies of light waves have become common with mode-locked laser frequency combs[1]. Despite their huge success, optical frequency combs currently remain bulky and expensive laboratory devices. Integrated photonic microresonators are promising candidates for comb generators in out-of-the-lab applications, with the potential for reductions in cost, power consumption and size[2]. Such advances will significantly impact fields ranging from spectroscopy and trace gas sensing[3] to astronomy[4], communications[5] and atomic time-keeping[6,7]. Yet, in spite of the remarkable progress shown over recent years[8–10], microresonator frequency combs ('microcombs') have been without the key function of direct *f*–2*f* self-referencing[1], which enables precise determination of the absolute frequency of each comb line. Here, we realize this missing element using a 16.4 GHz microcomb that is coherently broadened to an octave-spanning spectrum and subsequently fully phase-stabilized to an atomic clock. We show phase-coherent control of the comb and demonstrate its low-noise operation.

Focused research on microcombs has led to their realization in a growing range of materials and platforms[2,11–18]. Together with device development, much work has been aimed at the frequency control of microcombs[7,10,19–21], which is critical for many applications. However, full frequency stabilization of a self-referenced microcomb has not yet been demonstrated. The detection of microcomb offset frequencies has been problematic and could only be achieved using an additional reference frequency comb[19,22] or 2*f*–3*f* detection with transfer lasers[10]. Self-referencing is of particular importance because it provides direct measurement and control of the offset frequency of the microcomb and is key to forming a straightforward microwave-to-optical link. This is most simply implemented with an octave-spanning spectrum and a nonlinear *f*–2*f* interferometer to compare long and short wavelengths of the comb. Our work highlights coherent spectral broadening to an octave bandwidth to demonstrate *f*–2*f* self-referenced stabilization of the microcomb offset frequency and its mode-spacing at levels provided by state-of-the-art atomic clocks.

Figure 1a shows the experimental set-up for self-referencing of a microcomb. A tunable external cavity diode laser is amplified to ~100 mW and is coupled into a fused-silica microdisk resonator via a tapered optical fibre. The microdisk resonator[23] has a diameter of ~4 mm and a corresponding free spectral range of 16.4 GHz. The coupled linewidth of the resonator mode family for comb generation is 1.7 MHz, which yields a quality factor of $Q = 1.1 \times 10^8$ at the pump laser wavelength of 1,550 nm. The microresonator generates a phase-locked microcomb[24,25] with part of the comb light being detected by a fast photodiode to measure the repetition rate. The rest of the comb light is optimized in phase and amplitude using a liquid-crystal-based spatial light modulator to generate the shortest possible pulse at the input of a highly nonlinear fibre (HNLF 1 in Fig. 1a, input power ~150 mW). Note that this phase and amplitude optimization could be removed when using a single soliton microcomb generator, as demonstrated in Si_3N_4 and MgF_2 (refs 9,26). After another step of quadratic dispersion compensation and amplification to an average optical power of ~4 W, the 16.4 GHz pulse train of <200 fs pulses is sent into a second hybrid nonlinear optical fibre[27] that broadens the optical spectrum to an octave (Fig. 1b). The octave-spanning spectrum is sent to an *f*–2*f* interferometer for generation of the carrier envelope offset beat note. The *f*–2*f* interferometer includes a variable time delay for the long wavelength part of the spectrum in order to achieve a temporal overlap with the short wavelength end of the spectrum. Nonlinear frequency doubling of the 2.22 μm spectral region to 1.11 μm is achieved in a 10-mm-long periodically poled lithium niobate crystal. Both the measured repetition rate f_{rep} and carrier envelope offset frequency f_{ceo} are referenced to a hydrogen maser frequency reference. Feedback to the power and frequency of the pump laser allows stabilization of both f_{ceo} and f_{rep} of the microcomb. Figure 1c presents a photograph of the 4-mm-diameter fused-silica disk with tapered optical fibre that was used in this experiment.

Figure 2a shows the microcomb spectrum around a wavelength of 1.11 μm together with the frequency-doubled light from 2.22 μm measured with an optical spectrum analyser at a resolution bandwidth of 5 GHz. This resolution bandwidth allows the modes of the microcomb to be resolved and gives an estimate of the carrier envelope offset frequency of 7.5 GHz (frequency spacing between modes at 1.11 μm and frequency-doubled modes). The corresponding carrier envelope offset beat note (f_{ceo}) detected by interfering the fundamental and doubled light on a fast photodiode is shown in Fig. 2b, exhibiting 30 dB signal-to-noise at a resolution bandwidth of 100 kHz. Figure 2c shows a 25 min recording of the carrier envelope offset frequency and the corresponding Allan deviation. The microcomb f_{ceo} is stable at the 1% level over many weeks (when using the same pump mode and similar comb states). Significantly, we note that the free-running fractional stability of the microcomb f_{ceo} is comparable to the best solid-state laser frequency combs, even with no special attention given to environmental isolation at this point.

[1]National Physical Laboratory (NPL), Teddington TW11 0LW, UK. [2]National Institute of Standards and Technology (NIST), Boulder, Colorado 80305, USA. [3]T. J. Watson Laboratory of Applied Physics, California Institute of Technology, Pasadena, California 91125, USA. †Present addresses: Laboratoire Interdisciplinaire Carnot de Bourgogne, UMR CNRS 6303, 9 Avenue Alain Savary, 21078 Dijon, France (A.C.); Graduate School of Nanoscience and Technology, Korea Advanced Institute of Science and Technology, Daejeon 305-701, South Korea (H.L.).
*e-mail: pascal.delhaye@npl.co.uk; scott.diddams@nist.gov

© 2016 Macmillan Publishers Limited. All rights reserved

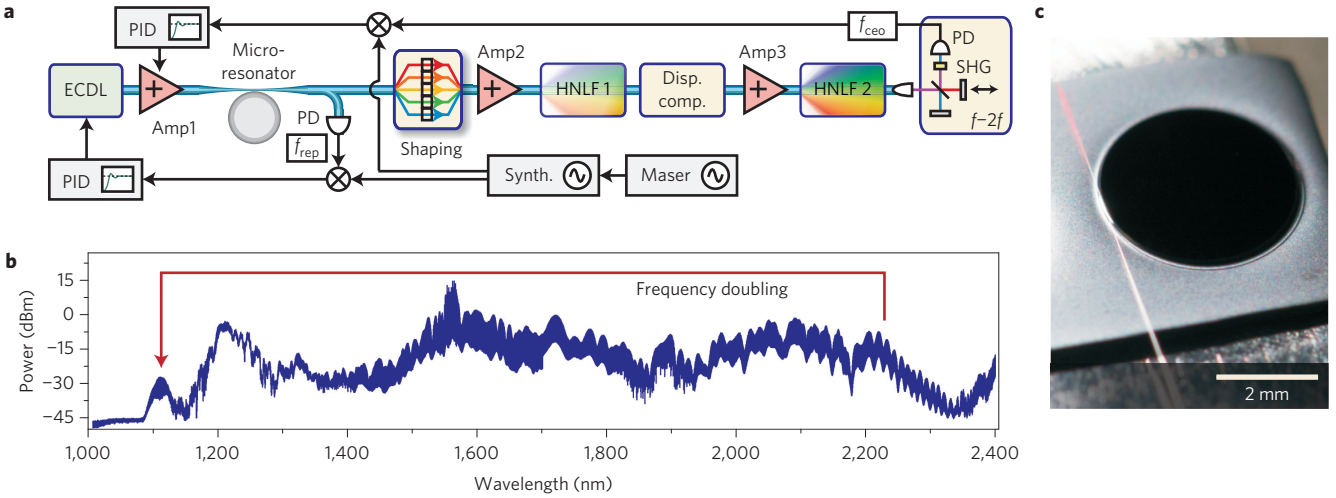

Figure 1 | Experimental set-up for *f*–2*f* self-referencing of a microcomb. a, The microcomb is generated by an amplified external cavity diode laser (ECDL) and phase-optimized for the generation of Fourier-limited pulses shorter than 200 fs. Subsequent amplification and broadening in highly nonlinear fibre (HNLF) generates an octave-spanning comb spectrum and enables the measurement of the carrier envelope offset frequency (f_{ceo}) using an *f*–2*f* interferometer. Repetition rate f_{rep} and carrier envelope offset f_{ceo} of the microcomb can be stabilized to an atomic clock (hydrogen maser). Amp, erbium-doped fibre amplifier; PD, photodiode; PID, proportional-integral-derivative controller; 'Shaping', liquid-crystal-based spatial light modulator; SHG, second harmonic generation. **b**, Octave-spanning microcomb spectrum after nonlinear broadening. **c**, Photograph of the 4-mm-diameter SiO_2 disk used in the experiment.

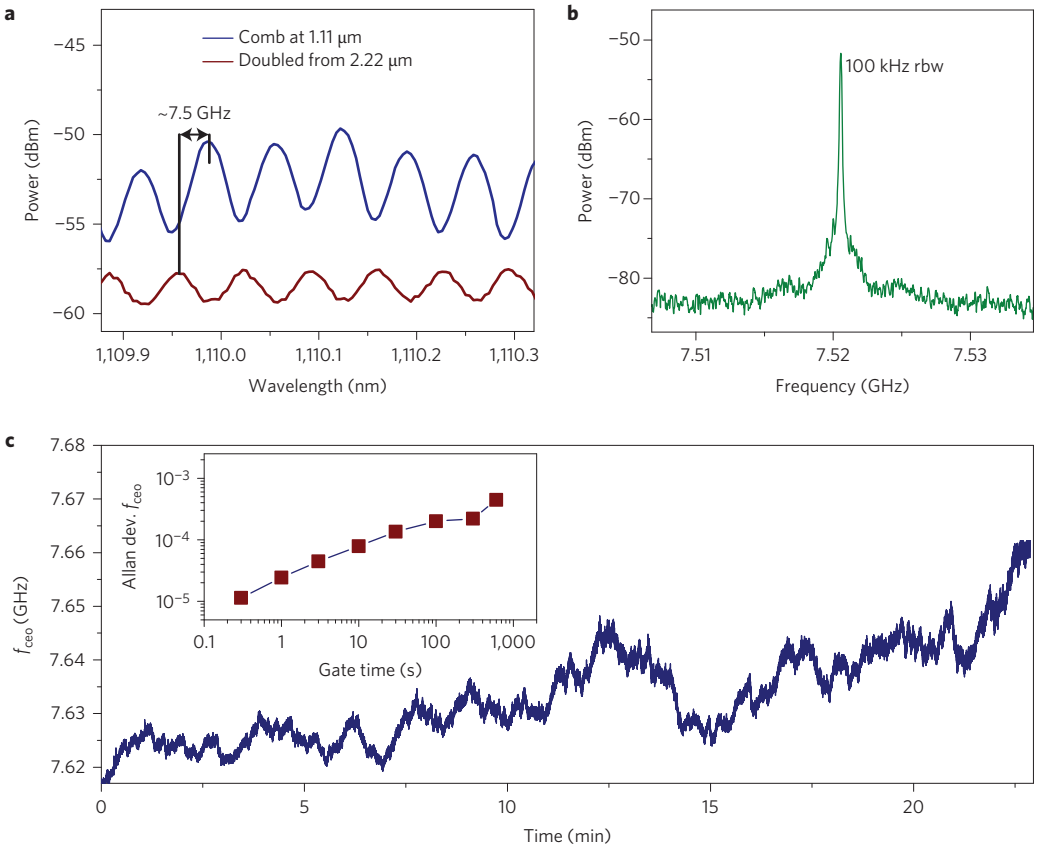

Figure 2 | Carrier envelope offset frequency measurement. a, Measurement of microcomb modes around a wavelength of 1.11 μm together with frequency-doubled comb modes originating from 2.22 μm wavelength. The carrier envelope offset frequency of ~7.5 GHz can be resolved as the offset between the fundamental and frequency-doubled comb modes (spectrum analyser resolution bandwidth of ~5 GHz). **b**, Electronic spectrum of the carrier envelope offset beat note with a signal-to-noise of >30 dB. rbw, resolution bandwidth. **c**, Time series measurement of the free-running carrier envelope offset frequency. The drift is attributed to laboratory temperature fluctuations and pump laser power/frequency drifts. Inset: Allan deviation of f_{ceo} normalized to the 16.4 GHz repetition rate.

© 2016 Macmillan Publishers Limited. All rights reserved

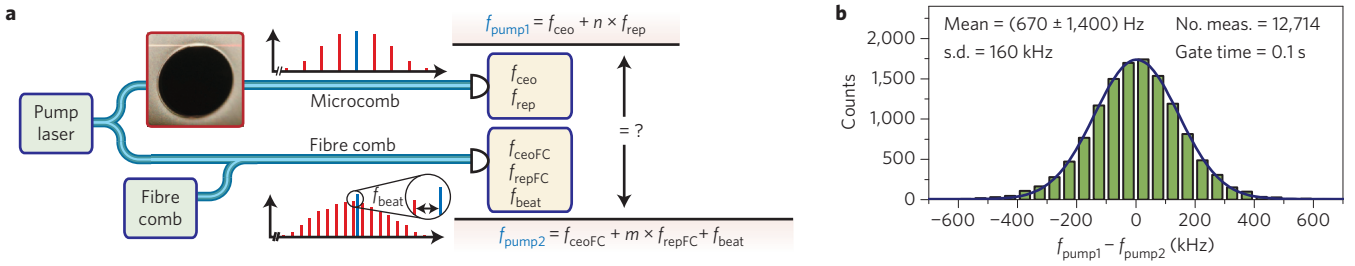

Figure 3 | Absolute optical frequency measurement and out-of-loop validation. a, Set-up diagram. The free-running pump laser frequency is determined by measuring the microcomb carrier envelope offset frequency and repetition rate. It is measured simultaneously with a conventional fibre laser frequency comb. **b**, Histogram showing the agreement of the free-running pump laser frequency measurements at a measurement time limited level of 670 Hz ± 1.4 kHz.

To verify the measurement of the actual carrier envelope offset frequency of the microcomb, we compared the frequency of the pump laser with an independent measurement using a self-referenced erbium:fibre frequency comb. The optical frequency of the pump laser was determined from the microcomb's repetition rate f_{rep} and carrier envelope offset frequency f_{ceo}

$$f_{pump1} = f_{ceo} + n \times f_{rep} \quad (1)$$

where n is an integer number corresponding to the mode number of the pump laser. In addition, the pump laser frequency measured with the erbium:fibre frequency comb with carrier envelope offset frequency f_{ceoFC} and repetition rate f_{repFC} yields

$$f_{pump2} = f_{ceoFC} + m \times f_{repFC} + f_{beat} \quad (2)$$

Here, m is the mode number of the closest fibre comb mode to the pump laser and f_{beat} is the measured beat note frequency between the pump laser and the closest fibre comb mode. Figure 3 shows an illustration of the measurement and a plot of the measured differences between f_{pump1} and f_{pump2}. Note that this measurement was acquired with a microcomb repetition rate and carrier envelope offset frequency free running. The microcomb's carrier envelope offset frequency was measured using the peak finder function of a maser-referenced electronic spectrum analyser. This allowed us to measure a carrier envelope offset frequency beat note with very small signal-to-noise (<5 dB) with a measurement rate exceeding 100 samples per second at a resolution bandwidth of 20 kHz in fast Fourier transform (FFT) mode (long-term direct f_{ceo} counting measurements were too unreliable because of insufficient signal-to-noise). Note that the scatter of ~160 kHz of the frequency measurement is due to the timing synchronization between measuring the free-running f_{ceo} and f_{rep} of the microcomb. The agreement between the measurements of the pump laser frequency with the microcomb and the fibre laser comb is 670 Hz ± 1.4 kHz, limited by the measurement time. Stabilization of the microcomb significantly improves the measurement accuracy, as is shown in the remaining part of this Letter.

Figure 4 presents a block diagram of a set-up that is used to stabilize the carrier envelope offset frequency of the microcomb. The initial carrier envelope offset beat note at 7.5 GHz is amplified and mixed down to ~640 MHz using a hydrogen maser referenced synthesizer. In the next step, the signal is divided by 64 and phase-locked to a maser-referenced 10 MHz signal. The error signal for the phase-locked loop is generated in a digital phase comparator and fed into a proportional-integral-derivative controller. Control of the carrier envelope offset frequency is achieved by actuating on the power (via Amp1, Fig. 1a) or frequency of the pump laser. Both these actuators change the intracavity power and detuning between the microresonator mode and pump laser. This effectively changes both the comb spacing and carrier envelope offset

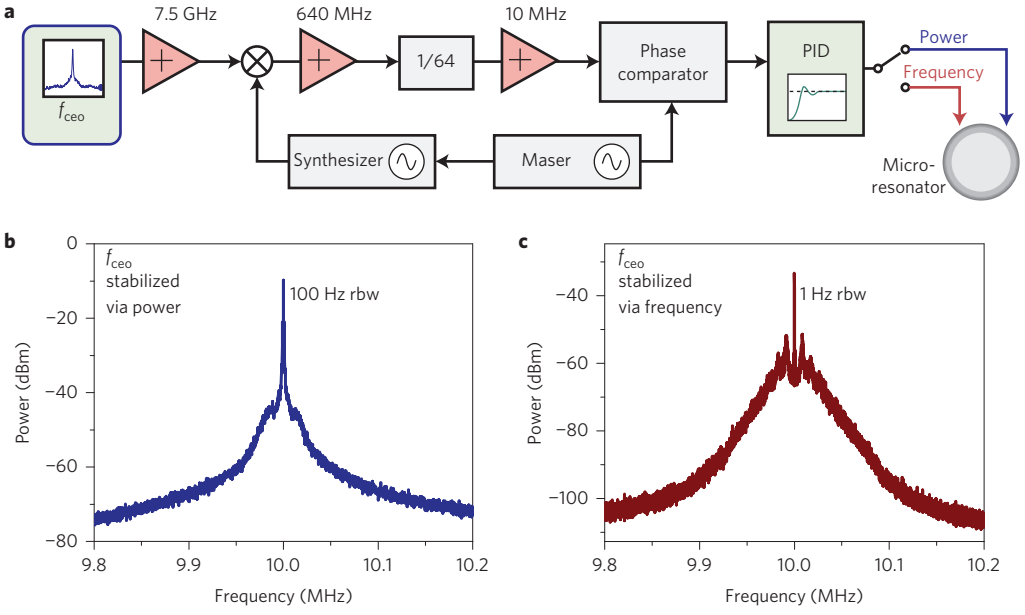

Figure 4 | Carrier envelope offset frequency stabilization. a, Block diagram of the electronic set-up for microcomb carrier envelope offset stabilization. **b**,**c**, The stabilized carrier envelope offset beat note using pump power (**b**) and pump frequency (**c**) as actuator. rbw, resolution bandwidth.

© 2016 Macmillan Publishers Limited. All rights reserved

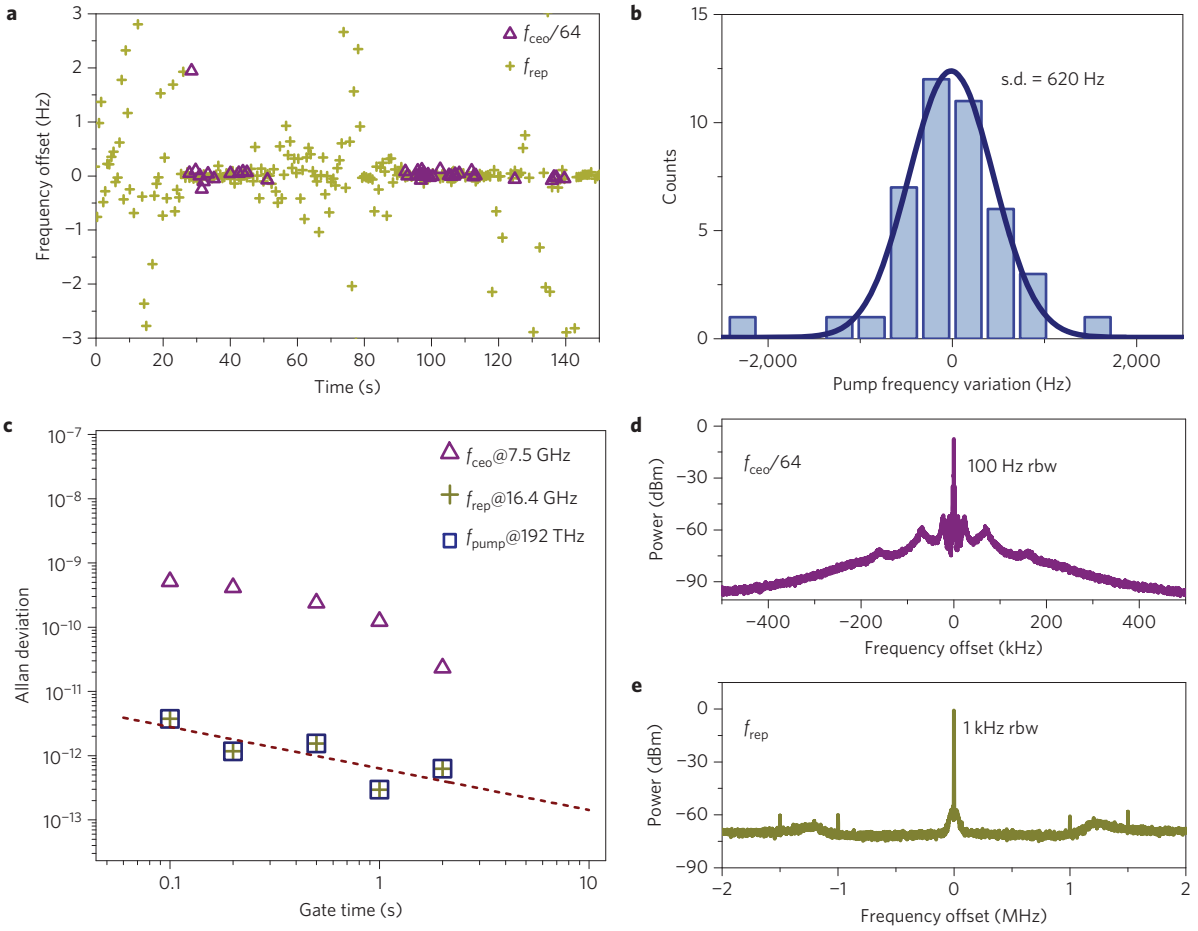

Figure 5 | Stabilizing a self-referenced microcomb to a hydrogen maser frequency reference. a, Simultaneous stabilization of carrier envelope offset frequency and repetition rate. Plotted are the counted in-loop signals of $f_{ceo}/64$ and f_{rep}. To maintain stable comb generation the actuation range is reduced, leading to a limited 'catch range' of the frequency lock. **b**, Histogram of the measured pump laser frequency with a standard deviation of 620 Hz at 100 ms gate time. **c**, Allan deviations of f_{ceo}, f_{rep} and f_{pump}. The pump laser frequency measurement is limited by the repetition rate stabilization, which is multiplied by the pump laser mode number of ~12,000. The red dashed line is a least-squares fit of the pump laser Allan deviation. **d**, Stabilized carrier envelope offset frequency beat note after mixing down and dividing by 64. **e**, Stabilized repetition rate beat note. rbw, resolution bandwidth.

frequency via fast thermal effects and the Kerr effect[19]. Figure 4b,c presents in-loop measurements of the stabilized carrier envelope offset frequency beat notes (after mixing down to 640 MHz and dividing by 64) for stabilization via pump power and pump frequency, respectively. The sharp carrier peaks indicate phase-locked control relative to the 10 MHz maser signal.

Full stabilization of the microcomb is achieved by using the pump laser frequency to control the comb spacing and the pump power to control the carrier envelope offset frequency. This configuration has been chosen to minimize crosstalk between the actuators. The amount of crosstalk between repetition rate and offset frequency control is observed to depend on coupling conditions. More specifically we observed inversion points of the repetition rate with respect to the pump power that significantly reduced the crosstalk. Figure 5a shows a simultaneous frequency counter measurement of both $f_{ceo}/64$ and f_{rep} compared to their set-points. Note that the employed phase-locked microcomb state only allowed for a limited variation in pump power and pump frequency, which leads to a limited 'capture-range' of the phase-locked loop (this could be improved by better environmental control and by using more robust comb states). Nevertheless, we were able to stabilize both degrees of freedom of the microcomb simultaneously to a sub-hertz residual noise level (at 1 s gate time). Based on these measurements, we calculated the absolute pump laser stability with a standard deviation of 620 Hz at a 100 ms gate time, which is consistent with the stability of the employed hydrogen maser references. Figure 5c shows the Allan deviation for f_{ceo}, f_{rep} and the pump laser frequency calculated as $f_{pump} = f_{ceo} + 11{,}709 \times f_{rep}$. This shows that the pump laser stability is mostly limited by repetition rate fluctuations due to the large multiplicative factor. At 1 s gate time, the carrier envelope offset frequency is stabilized to a sub-hertz level and only contributes at the 10^{-14} level to the optical carrier stability. Figure 5d,e show the stabilized and maser-referenced beat notes of $f_{ceo}/64$ and f_{rep}, respectively. Note that the carrier envelope offset frequency exhibits additional side lobes at a frequency offset of ~80 kHz, which arise from crosstalk with the repetition-rate phase-locked loop.

In conclusion, we have demonstrated f–$2f$ self-referencing of a microresonator-based optical frequency comb at a repetition rate of 16.4 GHz. The carrier envelope offset frequency is controlled via the pump laser power and frequency. Moreover, we simultaneously stabilize the carrier envelope offset frequency and repetition rate to a hydrogen maser-based atomic clock frequency reference. A self-referenced measurement of the pump laser frequency with an out-of-loop comparison with a conventional frequency comb confirms the viability of microcombs for metrology

© 2016 Macmillan Publishers Limited. All rights reserved

applications. Looking forward, our demonstration of external broadening of the microcomb spectrum can take advantage of chip-integrated highly nonlinear waveguides[28,29] to realize micro-photonic self-referenced optical frequency comb systems. Taken together with progress in the generation of low-noise soliton states[9,26], advanced dispersion engineering[15,18,30,31] and octave-span dispersive wave generation, these results highlight the future direction of chip-integrated microcombs as phase-coherent microwave-to-optical links.

Received 12 January 2016; accepted 27 April 2016;
published online 6 June 2016

References

1. Udem, T., Holzwarth, R. & Hänsch, T. W. Optical frequency metrology. *Nature* **416,** 233–237 (2002).
2. Del'Haye, P. *et al.* Optical frequency comb generation from a monolithic microresonator. *Nature* **450,** 1214–1217 (2007).
3. Diddams, S. A., Hollberg, L. & Mbele, V. Molecular fingerprinting with the resolved modes of a femtosecond laser frequency comb. *Nature* **445,** 627–630 (2007).
4. Steinmetz, T. *et al.* Laser frequency combs for astronomical observations. *Science* **321,** 1335–1337 (2008).
5. Pfeifle, J. *et al.* Optimally coherent Kerr combs generated with crystalline whispering gallery mode resonators for ultrahigh capacity fiber communications. *Phys. Rev. Lett.* **114,** 093902 (2015).
6. Savchenkov, A. A. *et al.* Stabilization of a Kerr frequency comb oscillator. *Opt. Lett.* **38,** 2636–2639 (2013).
7. Papp, S. B. *et al.* Microresonator frequency comb optical clock. *Optica* **1,** 10–14 (2014).
8. Coen, S., Randle, H. G., Sylvestre, T. & Erkintalo, M. Modeling of octave-spanning Kerr frequency combs using a generalized mean-field Lugiato–Lefever model. *Opt. Lett.* **38,** 37–39 (2013).
9. Herr, T. *et al.* Temporal solitons in optical microresonators. *Nature Photon.* **8,** 145–152 (2013).
10. Jost, J. D. *et al.* Counting the cycles of light using a self-referenced optical microresonator. *Optica* **2,** 706–711 (2015).
11. Savchenkov, A. A. *et al.* Tunable optical frequency comb with a crystalline whispering gallery mode resonator. *Phys. Rev. Lett.* **101,** 093902 (2008).
12. Levy, J. S. *et al.* CMOS-compatible multiple-wavelength oscillator for on-chip optical interconnects. *Nature Photon.* **4,** 37–40 (2010).
13. Razzari, L. *et al.* CMOS-compatible integrated optical hyper-parametric oscillator. *Nature Photon.* **4,** 41–45 (2010).
14. Ferdous, F. *et al.* Spectral line-by-line pulse shaping of on-chip microresonator frequency combs. *Nature Photon.* **5,** 770–776 (2011).
15. Grudinin, I. S. & Yu, N. Dispersion engineering of crystalline resonators via microstructuring. *Optica* **2,** 221–224 (2015).
16. Jung, H., Xiong, C., Fong, K. Y., Zhang, X. F. & Tang, H. X. Optical frequency comb generation from aluminum nitride microring resonator. *Opt. Lett.* **38,** 2810–2813 (2013).
17. Hausmann, B., Bulu, I., Venkataraman, V., Deotare, P. & Loncar, M. Diamond nonlinear photonics. *Nature Photon.* **8,** 369–374 (2014).
18. Yang, K. *et al.* Broadband dispersion-engineered microresonator on a chip. *Nature Photon.* **10,** 316–320 (2016).
19. Del'Haye, P., Arcizet, O., Schliesser, A., Holzwarth, R. & Kippenberg, T. J. Full stabilization of a microresonator-based optical frequency comb. *Phys. Rev. Lett.* **101,** 053903 (2008).
20. Papp, S. B., Del'Haye, P. & Diddams, S. A. Mechanical control of a microrod-resonator optical frequency comb. *Phys. Rev. X* **3,** 031003 (2013).
21. Del'Haye, P., Papp, S. B. & Diddams, S. A. Hybrid electro-optically modulated microcombs. *Phys. Rev. Lett.* **109,** 263901 (2012).
22. Jost, J. *et al.* All-optical stabilization of a soliton frequency comb in a crystalline microresonator. *Opt. Lett.* **40,** 4723–4726 (2015).
23. Lee, H. *et al.* Chemically etched ultrahigh-*Q* wedge-resonator on a silicon chip. *Nature Photon.* **6,** 369–373 (2012).
24. Del'Haye, P., Beha, K., Papp, S. B. & Diddams, S. A. Self-injection locking and phase-locked states in microresonator-based optical frequency combs. *Phys. Rev. Lett.* **112,** 043905 (2014).
25. Del'Haye, P. *et al.* Phase steps and resonator detuning measurements in microresonator frequency combs. *Nature Commun.* **6,** 5668 (2015).
26. Brasch, V. *et al.* Photonic chip-based optical frequency comb using soliton Cherenkov radiation. *Science* **351,** 357–360 (2016).
27. Beha, K. *et al.* Self-referencing a continuous-wave laser with electro-optic modulation. Preprint at http://arxiv.org/abs/1507.06344 (2015).
28. Kuyken, B. *et al.* An octave-spanning mid-infrared frequency comb generated in a silicon nanophotonic wire waveguide. *Nature Commun.* **6,** 6310 (2015).
29. Mayer, A. S. *et al.* Frequency comb offset detection using supercontinuum generation in silicon nitride waveguides. *Opt. Express* **23,** 15440–15451 (2015).
30. Del'Haye, P. *Optical Frequency Comb Generation in Monolithic Microresonators*. PhD thesis, Ludwig Maximilian Univ. Munich (2011).
31. Del'Haye, P., Arcizet, O., Gorodetsky, M. L., Holzwarth, R. & Kippenberg, T. J. Frequency comb assisted diode laser spectroscopy for measurement of microcavity dispersion. *Nature Photon.* **3,** 529–533 (2009).

Acknowledgements

This work is supported by the National Institute of Standards and Technology, the National Physical Laboratory, the California Institute of Technology, the Defense Advanced Research Projects Agency Quantum—Assisted Sensing and Readout programme, the Air Force Office of Scientific Research and the National Aeronautics and Space Administration. P.D. acknowledges support from the Humboldt Foundation. D.C.C. acknowledges support from the National Science Foundation Graduate Research Fellowship Program under grant no. DGE 1144083.

Author contributions

P.D., S.B.P. and S.A.D. conceived the experiments. P.D. and A.C. designed and performed the experiments. T.F. contributed to the f_{ceo} stabilization. K.B. and D.C.C. contributed to the nonlinear spectral broadening. K.Y.Y., H.L. and K.J.V. provided the microresonator. P.D. and S.A.D. prepared the manuscript, with input from all co-authors.

Additional information

Reprints and permissions information is available online at www.nature.com/reprints. Correspondence and requests for materials should be addressed to P.D. and S.A.D.

Competing financial interests

The authors declare no competing financial interests.

© 2016 Macmillan Publishers Limited. All rights reserved